Patterning of chemical gradients with submicrometer resolution using edge-spreading lithography

Geissler, Matthias; Chalsani, Preeti; Cameron, Neil S.; Veres, Teodor

Publisher's version / la version de l'éditeur:
Small, 2, 6, pp. 760-765, 2006-04-25

Web page / page Web
http://dx.doi.org/10.1002/smll.200600064
http://nparc.cisti-icist.nrc-cnrc.gc.ca/npsi/ctrl?action=rtdoc&an=15878010&lang=en
http://nparc.cisti-icist.nrc-cnrc.gc.ca/npsi/ctrl?action=rtdoc&an=15878010&lang=fr

Lithographic techniques

DOI: 10.1002/smll.200600064

Patterning of Chemical Gradients with Submicrometer Resolution Using Edge-Spreading Lithography**

Matthias Geissler, Preeti Chalsani, Neil S. Cameron, and Teodor Veres*

The development of methods for patterning chemical gradients on substrates has gained much attention in recent years. Inspired by their prevalence in nature, gradient surfaces are now being engineered and used as model substrates in several areas since they conveniently allow for probing the effects of surface energy and surface composition on a variety of interfacial phenomena such as wetting, nucleation, and adhesion. In biology, for example, gradients have served as templates to investigate optimal surface conditions for cellular attachment, proliferation, growth, migration, or phenotype changes.[1] The methodology of patterning surface gradients can vary depending on the materials involved and the resolution to be achieved.[2–12]

Self-assembled monolayers (SAMs) – ordered and dense layers of molecules adsorbed on a surface – are exquisite systems for introducing functionality to substrates in a chemically defined way and are thus well suited for gradient fabrication. For example, Chaudhury and Whitesides have prepared macroscopic-gradient SAMs on silicon substrates by controlling the diffusion of an alkyltrichlorosilane through the vapor phase.[6] Liedberg and co-workers have used cross diffusion of two different alkanethiols from opposite sides of a polysaccharide matrix to produce SAM gradients on gold substrates.[7] More recently, Efimenko and Genzer have shown that controlled deformation can be used to tune the grafting density of a silane on the surface of a flexible support.[8] A relatively simple method reported by Morgenthaler et al. relies on the gradual immersion of a gold substrate in a solution of alkanethiols.[9] The inverse approach, that is, the gradual desorption of thiols from a gold substrate, was demonstrated by Bohn and co-workers who applied a nonuniform electrochemical potential to a SAM-covered gold electrode.[10] The formation of gradient SAMs using microcontact printing has been shown by using curved or tapered poly(dimethylsiloxane) (PDMS) stamps to induce an unisotropic delivery of ink molecules to a substrate.[11] While the lateral dimensions of the gradients being fabricated using the preceding techniques range from micro- to centimeter length scales, the formation of submicrometer gradient SAMs remains challenging. One solution was demonstrated by Gorman and co-workers using replacement lithography mediated by a scanning tunneling microscope.[12]

In this paper, we describe a simple and flexible approach for patterning gradient SAMs of alkanethiols on gold substrates using the technique of edge-spreading lithography (ESL).[13] In contrast to most other techniques, a multitude of gradient features can be patterned on the same substrate in a parallel fashion while providing both control over the composition of the gradients and high resolution. There are two key features of ESL: A relief (or guiding) structure that needs to be present on the gold substrate, and reactive spreading. The role of the relief structure is to mediate the transport of alkanethiol molecules from a PDMS stamp to the gold surface and to determine the geometry of the emerging SAM. For example, when a two-dimensional (2D) array of silica beads is used, the circular footprint of each bead produces a pattern of monolayer rings in a hexagonal arrangement.[13c] Reactive spreading is the expansion of a SAM across a surface driven by a chemical reaction between molecules and the substrate;[14] it can only occur when an excess of unbound, SAM-forming molecules, and an unoccupied area on the surface into which the SAM can expand are both available. The edges of the emerging monolayer serve as nucleation sites that the molecules reach by diffusion. Using this effect, one can pattern multiple alkanethiolate SAMs on gold in a side-by-side arrangement by performing successive prints on the same substrate.[13a] In the present demonstration, we extend the concept of ESL and show how competitive spreading of a binary alkanethiol mixture can be used to gradually alter the composition of SAMs on gold substrates at submicrometer length scales.

Figure 1 illustrates the ESL procedure for the patterning of a gradient using a 1:1 mixture of 16-mercaptohexadecanoic acid (MHA, $HS(CH_2)_{15}COOH$) and 1-octadecanethiol (ODT, $HS(CH_2)_{17}CH_3$). We selected these compounds because they a) form stable and well-defined monolayers on gold, b) are commercially available and compatible with standard inking and printing procedures, and c) provide terminal groups that are chemically distinct. Our process begins with the preparation of an appropriate substrate; here, a thin film of gold onto which a 2D array of silica beads (1.6 μm in diameter) was deposited. Such arrays were advantageous for a number of reasons: They can be formed easily, provide sufficient mechanical robustness, offer a high density of features per surface area, promote the diffusion of thiols, and, finally, can be removed by sonication without leaving notable residues on the surface. We inked a PDMS stamp with a binary mixture of MHA and ODT in ethanol, and brought it into contact with the silica beads. The thiol molecules diffused from the stamp to the gold via the surface of each bead leading to the formation of a mixed monolayer ring on the substrate. The SAM expanded outward in a radial fashion via reactive spreading for at least as long as contact between the stamp and the array was maintained. We hypothesized that a gradual change in the com-

[*] Dr. M. Geissler, Dr. P. Chalsani, Dr. N. S. Cameron, Dr. T. Veres
Conseil National de Recherches Canada
Institut des Matériaux Industriels
75 Boulevard de Mortagne, Boucherville, QC J4B 6Y4 (Canada)
Fax: (+1) 450 641-5105
E-mail: matthias.geissler@cnrc-nrc.gc.ca

[**] M.G. thanks Joseph M. McLellan and Prof. Younan Xia (University of Washington) for useful discussions and technical assistance. We are grateful to Michel M. Dumoulin (IMI/CNRC) for his support.

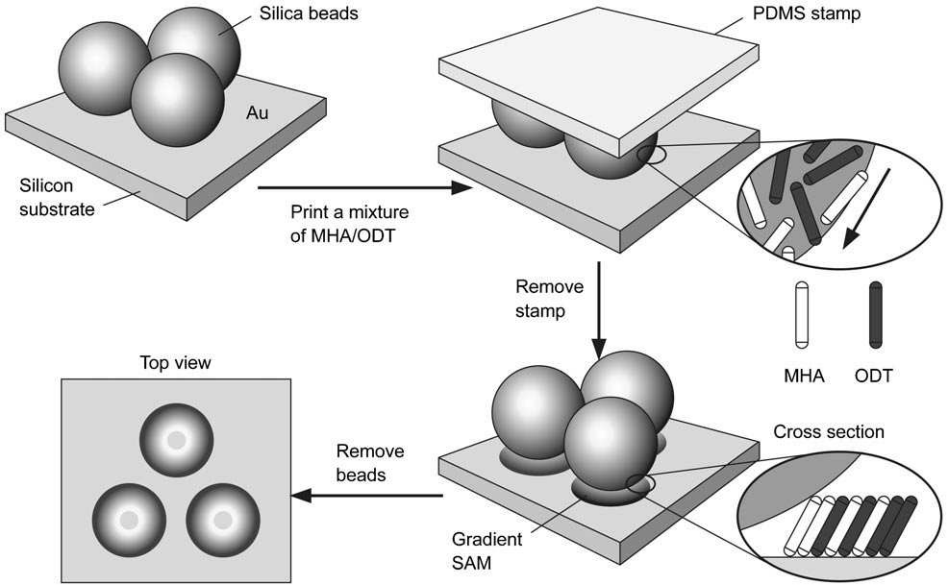

Figure 1. Schematic illustration of the ESL process used for patterning an array of gradient monolayer rings on a gold substrate. A PDMS stamp was inked with a mixture of MHA (bright) and ODT (dark), and printed onto a 2D array of silica beads immobilized on a thin film of gold. Molecules were released from the stamp during contact, and diffused along the surface of each bead. Upon reaching the gold substrate the molecules assembled into monolayer rings whose composition changed gradually from the inside to the outside (see text for details). Objects are not to scale.

position of the emerging SAM might be induced provided that the two thiols migrate at different rates, and there is no phase separation (i.e., domains forming within the SAM) during spreading.

To verify our hypothesis (Figure 2), we inked PDMS stamps with 1.0 mM solutions of MHA, ODT, or a mixture containing equimolar fractions (x) of the two ($x_{MHA} = x_{ODT} = 0.5$). These stamps were then printed onto 2D arrays of silica beads on gold substrates for 1, 1.5, 2, 3, and 4 min. After removing the beads from the substrate, we inspected the resultant SAM patterns using lateral force microscopy (LFM).[15] The MHA monolayer appears bright (Figure 2A) due to strong adhesive forces between the carboxyl groups and the hydrophilic surface of the silicon nitride tip. The ODT molecules, on the other hand, interact weakly with the tip, leading to a dark appearance of the ODT monolayer in the LFM images (Figure 2B). In both cases, the rings were homogeneous in color, which indicates a high uniformity across the entire width of the SAM. In contrast, the rings formed from a 1:1 mixture of MHA and ODT showed a gradual change in composition from the inside to the outside (Figure 2C and D). We consistently found that the inner portions of the rings were rich in MHA, while the outermost ones were dominated by ODT. Also, our findings suggest that that MHA and ODT molecules primarily coadsorbed into mixed phases rather than separated into their respective domains.[16]

The rate at which a SAM expands is defined by the overall time it takes for the molecules to diffuse from the stamp to the bare gold substrate. In a diffusive transport process, the mean displacement of a molecule ($<d^2>^{1/2}$) is related to the time (t) by $<d^2> = D \times t$, where D is the diffusion constant. In our case, the mean displacement of the molecules is also the average width of the corresponding monolayer rings. Figure 2E shows a plot of the ring width, that is, $<d^2>^{1/2}$ as a function of $t^{1/2}$ for SAMs formed from MHA, ODT, and a 1:1 mixture of MHA/ODT. For all three types of SAMs, we found a linear relationship between $<d^2>^{1/2}$ and $t^{1/2}$ as can be expected for the initial phases of SAM formation.[17] We estimated the diffusion constants from the slope of the fit curves and found that $D_{MHA} \approx 2.5 D_{ODT}$. The fact that MHA molecules diffuse faster than their ODT counterparts can hardly be explained in terms of molecular weight (288.49 versus 286.56 g mol^{-1} for MHA and ODT, respectively). Instead, we believe that this is a result of subtle differences in the interaction of the molecules with the PDMS stamp, the surface of silica beads, and the previously formed SAM, deriving from the distinct nature of their terminal functionalities. A detailed understanding of all the individual steps and processes (including possible depletion effects on the surface of the stamp) is yet to be achieved.

As we changed the value of x for the two compounds in the ink, the composition of the SAMs changed accordingly, allowing us to engineer gradients of variable composition and steepness (Figure 3). For example, when we increased x_{MHA} from 0.5 to 0.75, the resultant monolayers were dominated by MHA, and the composition of the SAMs changed more gradually, over a relatively long distance (Figure 3A). Decreasing x_{MHA} to 0.25 had the inverse effect: the SAMs were mainly composed of ODT, and their gradient portions were rather short and steep. It was not possible to quantify the local composition of the SAMs due to variations in the LFM signal intensities between different samples. However, we were able to make more meaningful assessments of the gradient composition by sandwiching the gradients between regions of pure SAMs by performing three subsequent prints on the same substrate. The example in Figure 3B shows a gradient in the form of three concentric rings obtained from printing a) MHA ($x_{MHA} = 1$), b) a 3:1 mixture of MHA/ODT ($x_{MHA} = 0.75$), and c) ODT ($x_{MHA} = 0$). Interestingly, the gradient was largely continuous between the first and the third segments. Reducing x_{MHA} in the ink (e.g., to 0.67 and below) resulted in gradients that typically showed a step in intensity between the first and the second ring (data not shown).

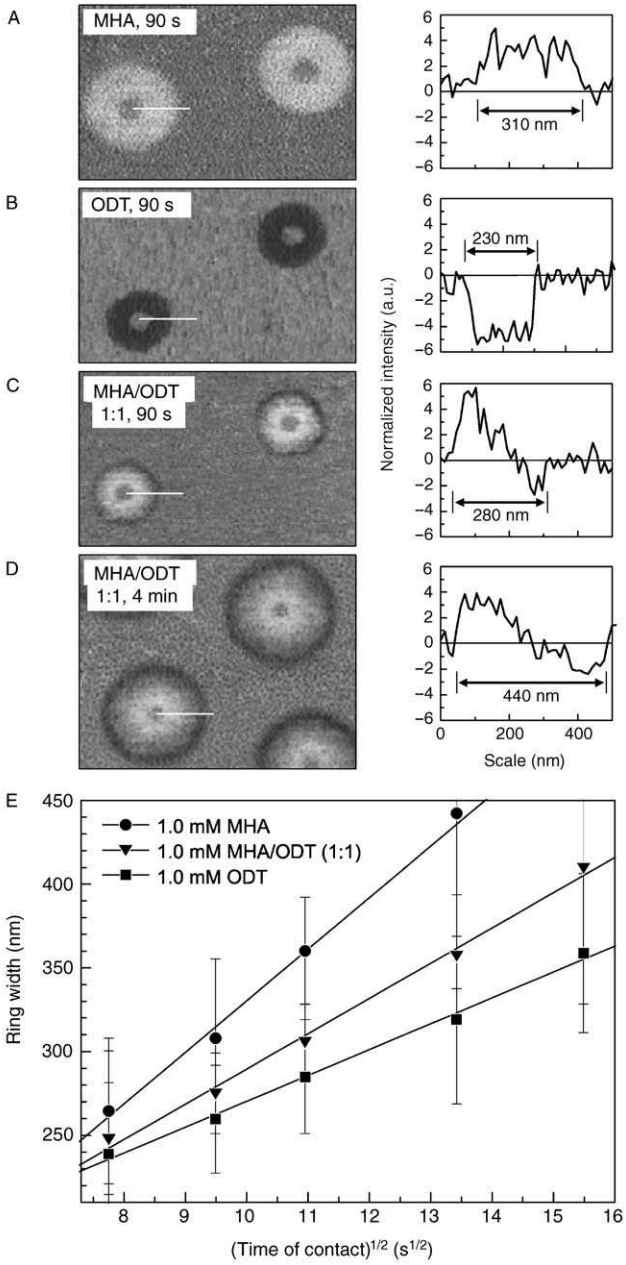

Figure 2. A–D) LFM images (left panel) and selected intensity plots (right panel) of monolayer rings patterned on gold substrates by ESL with MHA, ODT, and a 1:1 mixture of MHA/ODT, using silica beads (1.6 μm in diameter) as the guides. Note that the local composition and the steepness of the gradients changed slightly when the printing time was increased from 90 s (C) to 4 min (D). The white line in each image denotes 500 nm, and indicates the location of the corresponding intensity plot. E) A plot of the ring width versus printing time. Each data point was calculated from ≈10 randomly selected rings at several locations on a sample.

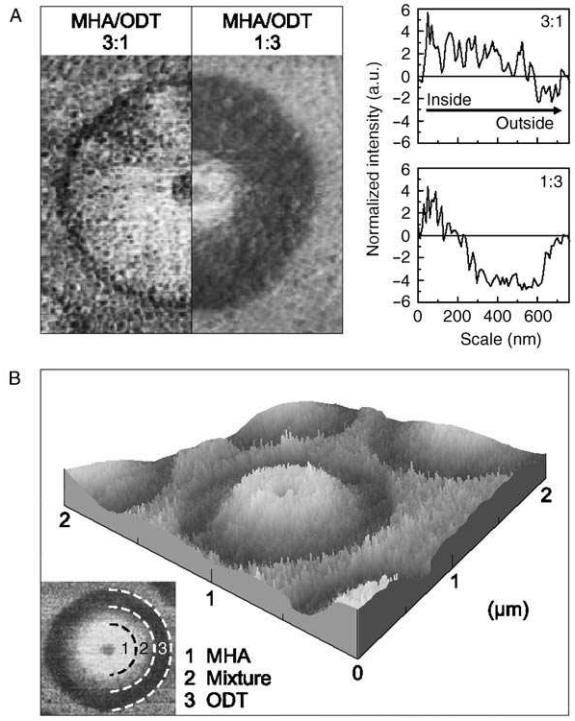

Figure 3. A) LFM images (left panel) and selected intensity plots (right panel) of gradients on gold that were formed by ESL using 3:1 and 1:3 mixtures of MHA/ODT. The total ink concentration was 1.0 mM, and the printing time was 8 min for both examples. B) LFM images of a gradient pattern that was obtained by performing three prints on the same substrate. The printing conditions were as follows: 1 min for MHA, 3 min for MHA/ODT ($x_{MHA} = 0.75$), and 6 min for ODT.

We performed a set of experiments in which we used our gradient surfaces as templates for the assembly of metallic nanoparticles (NPs) from a solution (Figure 4). The organization of particles into well-defined micro- and nanoscale structures at selected sites of a substrate – also known as colloidal epitaxy – has been the subject of extensive studies. The forces that govern the assembly process can vary depending on the size of the particles and their surface chemistry, and may include electrostatic interaction,[18] gravitation,[19] capillary action,[18b,19] hydrogen bonding,[20] and biomolecular recognition,[21] for example. The vast majority of demonstrations used substrates with uniform patterns; only a few published studies exist in which chemical gradients have been employed as templates for particle assembly.[22] We have synthesized two populations of NPs, namely, hydrophilic citrate-stabilized gold colloids and hydrophobic magnetic cobalt–iron oxide particles decorated with hydrocarbon ligands. According to the general rule *similia similibus solvuntur* ("like dissolves like"), we expected these NPs to show a preference in adsorption to either the hydrophilic or hydrophobic portions of a gradient SAM. The templates for our experiments were prepared by immersion of a gradient substrate (obtained from a 3:1 mixture of MHA and ODT) in a solution of ODT to complement each individual gradient ring, and to cover the bare regions of the gold surface with a SAM of ODT (Figure 4A). After incubation with either hydrophilic or hydrophobic particles, the samples were inspected by atomic force microscopy (AFM). The images in Figure 4B and C reveal striking results: Both types of NPs adsorbed with high selectivity forming density gradients on the substrate that followed the circular geometry of the monolayer rings. The hydrophilic gold NPs mainly

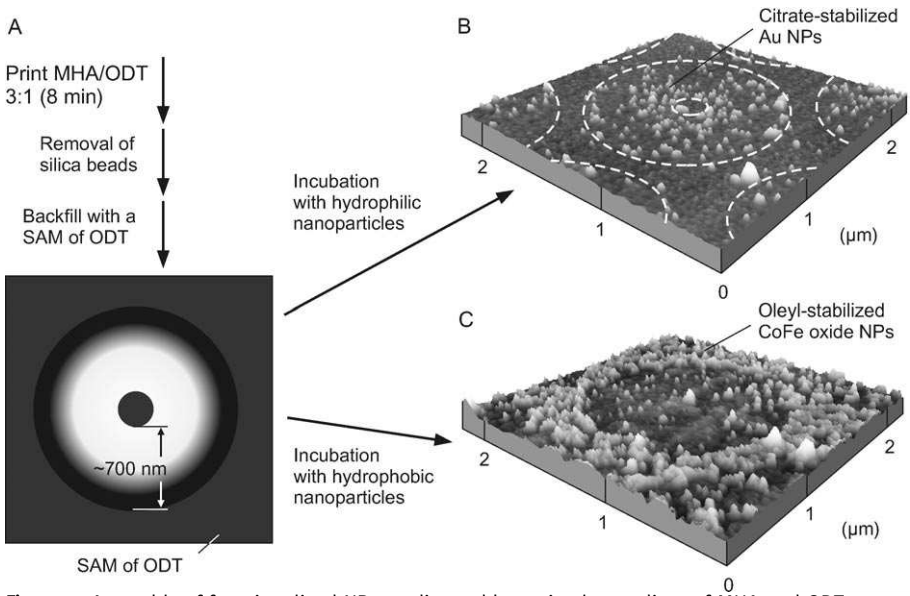

Figure 4. Assembly of functionalized NPs as directed by a circular gradient of MHA and ODT on a gold substrate. A) The preparation of the templates was carried out as follows: A PDMS stamp was inked with a 1.0 mM solution of MHA/ODT ($\chi_{MHA}=0.75$) and printed for 8 min onto silica beads (1.6 μm in diameter) immobilized on a gold substrate. After the beads were lifted off the substrate, the sample was immersed in a 1.0 mM solution of ODT for 90 min, which was followed by rinsing with ethanol and drying with a stream of nitrogen gas. The sample was then split in half and incubated with dilute solutions of hydrophilic and hydrophobic NPs, respectively. B, C) Three-dimensional AFM topography images showing the circular NP density gradients that formed on these templates. Note that the spot in the middle of the ring remained empty in the case of hydrophilic NPs (B), but was covered to a large extent when hydrophobic NPs (C) adsorbed on the substrate. The height scale is 100 nm in both images.

decorated the inner portions of the rings where the fraction of MHA was the highest. In contrast, hydrophobic NPs were largely absent from these inner regions, and preferentially adsorbed at those areas that were covered with the ODT monolayer. The surface density of the hydrophilic gold colloids was relatively low compared to that of their alkyl-stabilized CoFe oxide counterparts, which indicates subtle differences in the adhesion forces for these two NP species.

In summary, we have demonstrated a simple and convenient approach to direct the assembly of MHA and ODT molecules into gradient monolayer ring patterns on a gold substrate. Our method, which is essentially a bottom-up approach, involves the co-diffusion of these alkanethiols along the surface of silica beads immobilized on the gold substrate – a chromatography-like process that introduces a partial separation of the two species. LFM investigation of the monolayer rings emerging from the edges of each bead revealed that their inner portions primarily contained hydrophilic MHA molecules, while their outer regions mainly consisted of hydrophobic ODT molecules. We were able to alter the distribution of both thiol molecules in the SAM over length scales from 700 to 200 nm by varying either the mole fraction of MHA and ODT in the ink, or the printing time. In principle, variation of the sphere diameter should also affect the degree of separation between MHA and ODT molecules, and would therefore provide another means of tuning the slope of the gradients. Whether a change in surface chemistry of the beads has a similar effect on the composition of the SAM is difficult to predict and remains to be explored. While we validated the functionality of our patterns using the template-assisted assembly of NPs into circular density gradients, other applications including the formation of concentration gradients with proteins or DNA might also be possible.

Experimental Section

Preparation of substrates: Gold substrates were prepared by the thermal evaporation of 25 nm of gold (99.9999%, Alfa Aesar, Ward Hill, MA) onto a silicon wafer (Montco Silicon Technologies, Spring City, PA) that had been primed with 5 nm of chromium (99.95%, Alfa Aesar) using a 306 Thermoevaporator (BOC Edwards, Santa Clara, CA). The metals were deposited at a rate of ≈ 0.1 nm s^{-1} and a pressure of $\approx 2 \times 10^{-6}$ Torr. The gold-coated wafer was cut into pieces of ≈ 1 cm^2 in area, which were subjected to an air-plasma treatment (Harrick Scientific Corp., Pleasantville, NY) for 1 min to remove any possible organic contaminants. Monodispersed silica beads (1.57 ± 0.06 μm, suspended in water) were purchased from Duke Scientific Corp. (Palo Alto, CA). The commercial sample was diluted with deionized (DI) water (≈ 2 MΩ) to yield suspensions with ≈ 0.15% (w/w) bead content. Colloidal arrays were formed by placing 25 μL of the diluted suspension on a freshly cleaned gold substrate using a micropipette, and allowing the water to evaporate slowly.

Inking and printing: Planar PDMS slabs were prepared from Sylgard 184 (Dow Corning Corp., Midland, MI) by curing the mixed prepolymers of PDMS (elastomer base/curing agent = 10:1, w/w) on a flat polystyrene surface (Corning petri dish, Sigma–Aldrich Corp., St. Louis, MO) in an oven at 60 °C for ≈ 20 h. The PDMS slabs were cut into pieces of ≈ 1 cm^2 in area, which were used as stamps for inking and printing. MHA and ODT were both obtained from Sigma–Aldrich and purified by recrystallization from toluene (A&C American Chemicals Ltd., Montréal, QC) and ethanol (Commercial Alcohols Inc., Brampton, ON), respectively. During the purification process, solvents were purged with nitrogen gas to limit the formation of disulfides and other oxidized species. MHA and ODT were separately dissolved in ethanol to provide 1.0 mM stock solutions that were used to prepare the binary mixtures. All ink solutions were used within 24 h after their preparation to minimize aging effects. Stamps were inked by covering one side entirely with the ink for 1 min, followed by drying with a stream of nitrogen gas; they were then placed by hand onto a colloidal array for 1 to 8 min. After each

print, samples were allowed to rest for 1 to 3 min before further processing. Removal of the beads from the substrate was accomplished by sonication in DI water for ≈1 min followed by rinsing with isopropanol (Anachemia Canada Inc., Montréal, QC), and drying with a stream of nitrogen gas.

Nanoparticle synthesis and templated assembly: Hydrophilic gold NPs were prepared by the reductive precipitation of 5.0 mg (0.013 mmol) hydrogen tetrachloroaurate(III) (Strem Chemicals Inc., Newburyport, MA) in 50 mL of DI water with 15 mg (0.051 mmol) trisodium citrate (Sigma–Aldrich, added as a 34 mM aqueous solution) under reflux conditions.[23] Nucleation was observed within ≈30 s, and growth equilibrium was achieved within a few minutes. The resultant particles had an average diameter of 13±1 nm, as revealed by scanning transmission electron microscopy (STEM). Patterned gold substrates were incubated with a dilute gold NP solution (0.05%, w/w) for 90 min; they were then rinsed with DI water, and dried in air. Hydrophobic NPs were synthesized via cothermolysis of 1.8 g (7.0 mmol) cobalt(II) acetylacetonate (Sigma–Aldrich) and 1.3 g (6.0 mmol) iron pentacarbonyl (Sigma–Aldrich) in 40 mL diphenylether (Sigma–Aldrich) at reflux in the presence of 0.8 mL (3.0 mmol) oleylamine, 1.0 g (3.0 mmol) oleic acid, and 0.6 g (6.0 mmol) hexanediol (all obtained from Sigma–Aldrich), which served as stabilizing ligands.[24] The CoFe oxide NPs were precipitated with ethanol, centrifuged, and washed with hexanes (Fisher Scientific, Hampton, NH). Their average diameter was 29±2 nm according to STEM measurements. Patterned gold substrates were incubated with a dilute solution of hydrophobic NPs in hexanes (0.05%, w/w) for 5 min, rinsed with hexanes, and dried in air.

Instrumentation: AFM images were taken with a multimode Nanoscope IV atomic force microscope (Veeco Metrology Group, Santa Barbara, CA), operated at ambient conditions. LFM measurements were performed in contact mode using silicon nitride cantilevers (NP-S20, Veeco) with a spring constant of 0.12 $N\,m^{-1}$. For all images we recorded the trace direction of the tip using a scan angle of 90°. Cross-sectional intensity plots were normalized with respect to the gold substrate. For each friction force image, the overall offset of the data was adjusted so that the value of the bare gold substrate was at 0 mV. The measured intensity values were then normalized by the RMS roughness of the bare gold regions. The presented intensity plots correspond to a single-line scan; they only serve as illustrative examples since averaging over the circular geometry of our features was difficult to accomplish. Substrates decorated with NPs were imaged in tapping mode using silicon cantilevers (NanoWorld, Neuchâtel, Switzerland) with a spring constant of 42 $N\,m^{-1}$. All images were recorded at a rate of ≈1.0 Hz, and with a pixel resolution of 512. STEM inspection of NPs was accomplished with a Hitachi S-4800 scanning transmission electron microscope (Hitachi High-Technologies Canada, Rexdale, ON) operated at 30 keV, and by using Formvar-free carbon-coated copper grids (Marivac Inc., St.-Laurent, QC).

Keywords:
gradients · lateral force microscopy · monolayers · nanolithography · self-assembly

[1] a) R. R. Bhat, B. N. Chaney, J. Rowley, A. Liebmann-Vinson, J. Genzer, *Adv. Mater.* **2005**, *17*, 2802–2807; b) N. L. Jeon, H. Baskaran, S. K. W. Dertinger, G. M. Whitesides, L. Van De Water, M. Toner, *Nat. Biotechnol.* **2002**, *20*, 826–830; c) S. K. W. Dertinger, X. Jiang, Z. Li, V. N. Murthy, G. M. Whitesides, *Proc. Natl. Acad. Sci. USA* **2002**, *99*, 12542–12547.

[2] For gradient fabrication via plasma discharge, see: H. T. Spijker, R. Bos, W. van Oeveren, J. de Vries, H. J. Busscher, *Colloids Surf. B* **1999**, *15*, 89–97.

[3] The use of temperature gradients: a) Y. Liu, V. Klep, B. Zdyrko, I. Luzinov, *Langmuir* **2005**, *21*, 11806–11813; b) L. Ionov, M. Stamm, S. Diez, *Nano Lett.* **2005**, *5*, 1910–1914.

[4] The use of photochemical reactions with variation of the exposure dose: a) W. S. Dillmore, M. N. Yousaf, M. Mrksich, *Langmuir* **2004**, *20*, 7223–7231; b) I. Caelen, H. Gao, H. Sigrist, *Langmuir* **2002**, *18*, 2463–2467; c) C. B. Herbert, T. L. McLernon, C. L. Hypolite, D. N. Adams, L. Pikus, C.-C. Huang, G. B. Fields, P. C. Letourneau, M. D. Distefano, W.-S. Hu, *Chem. Biol.* **1997**, *4*, 731–737.

[5] Gradient fabrication with biomolecules using microfluidic devices: a) X. Jiang, Q. Xu, S. K. W. Dertinger, A. D. Stroock, T.-M. Fu, G. M. Whitesides, *Anal. Chem.* **2005**, *77*, 2338–2347; b) K. A. Fosser, R. G. Nuzzo, *Anal. Chem.* **2003**, *75*, 5775–5782; c) S. K. W. Dertinger, D. T. Chiu, N. L. Jeon, G. M. Whitesides, *Anal. Chem.* **2001**, *73*, 1240–1246; d) I. Caelen, A. Bernard, D. Juncker, B. Michel, H. Heinzelmann, E. Delamarche, *Langmuir* **2000**, *16*, 9125–9130; e) N. L. Jeon, S. K. W. Dertinger, D. T. Chiu, I. S. Choi, A. D. Stroock, G. M. Whitesides, *Langmuir* **2000**, *16*, 8311–8316.

[6] M. K. Chaudhury, G. M. Whitesides, *Science* **1992**, *256*, 1539–1541.

[7] a) M. Lestelius, I. Engquist, P. Tengvall, M. K. Chaudhury, B. Liedberg, *Colloids Surf. B* **1999**, *15*, 57–70; b) B. Liedberg, M. Wirde, Y.-T. Tao, P. Tengvall, U. Gelius, *Langmuir* **1997**, *13*, 5329–5334.

[8] K. Efimenko, J. Genzer, *Adv. Mater.* **2001**, *13*, 1560–1563.

[9] S. Morgenthaler, S. Lee, S. Zürcher, N. D. Spencer, *Langmuir* **2003**, *19*, 10459–10462.

[10] a) X. Wang, P. W. Bohn, *J. Am. Chem. Soc.* **2004**, *126*, 6825–6832; b) Q. Wang, P. W. Bohn, *J. Phys. Chem. B* **2003**, *107*, 12578–12584.

[11] a) T. Kraus, R. Stutz, T. E. Balmer, H. Schmid, L. Malaquin, N. D. Spencer, H. Wolf, *Langmuir* **2005**, *21*, 7796–7804; b) S.-H. Choi, B.-M. Z. Newby, *Langmuir* **2003**, *19*, 7427–7435.

[12] R. R. Fuierer, R. L. Carroll, D. L. Feldheim, C. B. Gorman, *Adv. Mater.* **2002**, *14*, 154–157.

[13] a) M. Geissler, J. M. McLellan, J. Chen, Y. Xia, *Angew. Chem.* **2005**, *117*, 3662–3666; *Angew. Chem. Int. Ed.* **2005**, *44*, 3596–3600; b) M. Geissler, J. M. McLellan, Y. Xia, *Nano Lett.* **2005**, *5*, 31–36; c) J. M. McLellan, M. Geissler, Y. Xia, *J. Am. Chem. Soc.* **2004**, *126*, 10830–10831.

[14] a) H. A. Biebuyck, G. M. Whitesides, *Langmuir* **1994**, *10*, 4581–4587; b) Y. Xia, G. M. Whitesides, *J. Am. Chem. Soc.* **1995**, *117*, 3274–3275; c) S. Rozhok, R. Piner, C. A. Mirkin, *J. Phys. Chem. B* **2003**, *107*, 751–757.

[15] a) G. J. Leggett, *Anal. Chim. Acta* **2003**, *479*, 17–38; b) R. W. Carpick, M. Salmeron, *Chem. Rev.* **1997**, *97*, 1163–1194.

[16] We could not elucidate the phase behavior of MHA and ODT on the molecular level. Several studies based on scanning tunneling microscopy suggest that nanometer-scale domains may form when alkanethiols co-adsorb from a solution onto a gold substrate. See, for example: S. J. Stranick, S. V. Atre, A. N. Parikh, M. C. Wood, D. L. Allara, N. Winograd, P. S. Weiss, *Nanotechnology* **1996**, *7*, 438–442. More recently, Mirkin and coworkers reported the near-complete phase-separation of MHA and ODT in mixed SAMs that were patterned by dip-pen nanolithography. See: K. Salaita, A. Amarnath, D. Maspoch, T. B. Hig-

gins, C. A. Mirkin, *J. Am. Chem. Soc.* **2005**, *127*, 11 283 – 11 287. We do not think that the findings of these authors are necessarily contradictory to ours as the transport mechanisms for the thiol molecules are somewhat different in these two methods.

[17] We performed our experiments in a clean room (class 1000) with semi-controlled temperature (19 ± 1 °C) and humidity (50 ± 10 %). However, the width of individual rings was prone to variation, as indicated by the relatively large error bars in the graph. In most cases, the ring width varied from one region to another on the same substrate, but was typically uniform within arrays. We believe that local variations in the population of beads on the gold substrate in conjunction with inking and printing artifacts primarily account for this finding.

[18] a) H. Zheng, M. F. Rubner, P. T. Hammond, *Langmuir* **2002**, *18*, 4505 – 4510; b) J. Aizenberg, P. V. Braun, P. Wiltzius, *Phys. Rev. Lett.* **2000**, *84*, 2997 – 3000.

[19] Y. Yin, Y. Lu, B. Gates, Y. Xia, *J. Am. Chem. Soc.* **2001**, *123*, 8718 – 8729.

[20] E. Hao, T. Lian, *Chem. Mater.* **2000**, *12*, 3392 – 3396.

[21] Y. C. Cao, R. Jin, C. A. Mirkin, *Science* **2002**, *297*, 1536 – 1540.

[22] a) S. T. Plummer, P. W. Bohn, *Langmuir* **2002**, *18*, 4142 – 4149; b) R. R. Bhat, D. A. Fischer, J. Genzer, *Langmuir* **2002**, *18*, 5640 – 5643.

[23] G. Frens, *Nature Phys. Sci.* **1973**, *241*, 20 – 22.

[24] S. Sun, H. Zeng, *J. Am. Chem. Soc.* **2002**, *124*, 8204 – 8205.

Received: February 6, 2006

